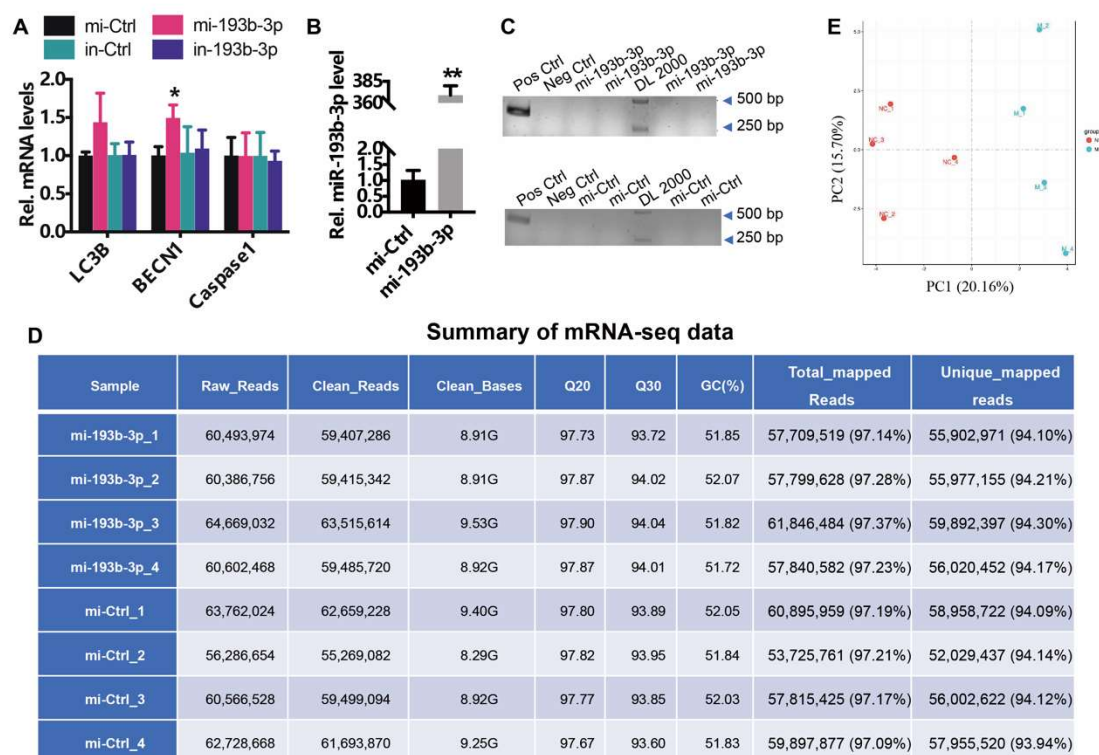


[illegible]

**Supplementary Figure S1 MIR193BHG expression from 53 human tissues.** Data are from GTEx (Release V6). A purple arrow marks the skeletal muscle.



## Supplementary Figure S2 Basic information for mRNA transcriptome in miR-193b-3p-treated MuSCs.

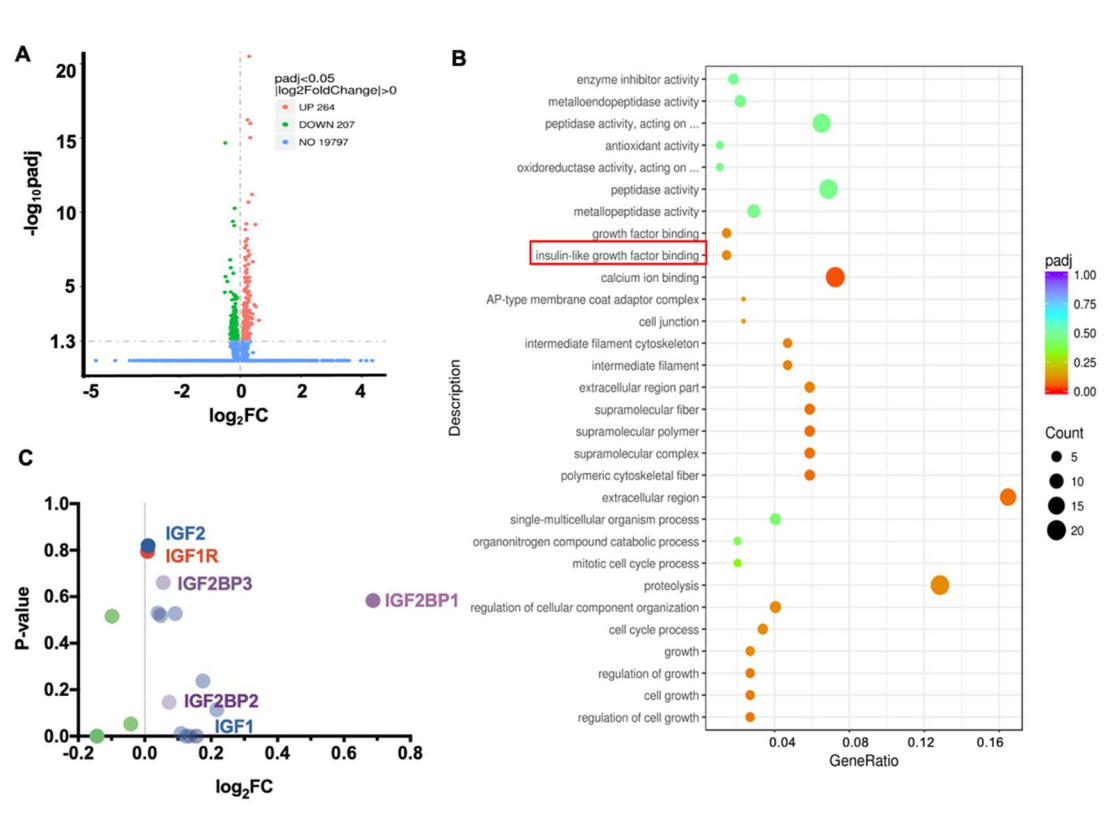
(A) Effect of miR-193b-3p on the transcripts of genes related to apoptosis and autophagy. The unpaired two-tailed t-test was used to evaluate the means difference. Data are shown as mean  $\pm$  MSE. \*  $P < 0.05$ .

(B) mi-193b-3p levels quantified using qPCR.

(C) Mycoplasma contamination in culturing media of samples (mi-193b-3p and mi-Ctrl-treated) detected using polymerase chain reaction (PCR) and subsequent 1.5% agarose gels electrophoresis, with the positive control (Pos Ctrl), negative control (Neg Ctrl), and DNA ladder DL2000.

(D) The basic information for the poly<sup>A</sup> mRNA-seq output data.

(E) Transcriptome clustering based on principal component analysis (PCA). The red dot represents control (NC), and the green dot represents miR-193b-3p mimics treated sample.



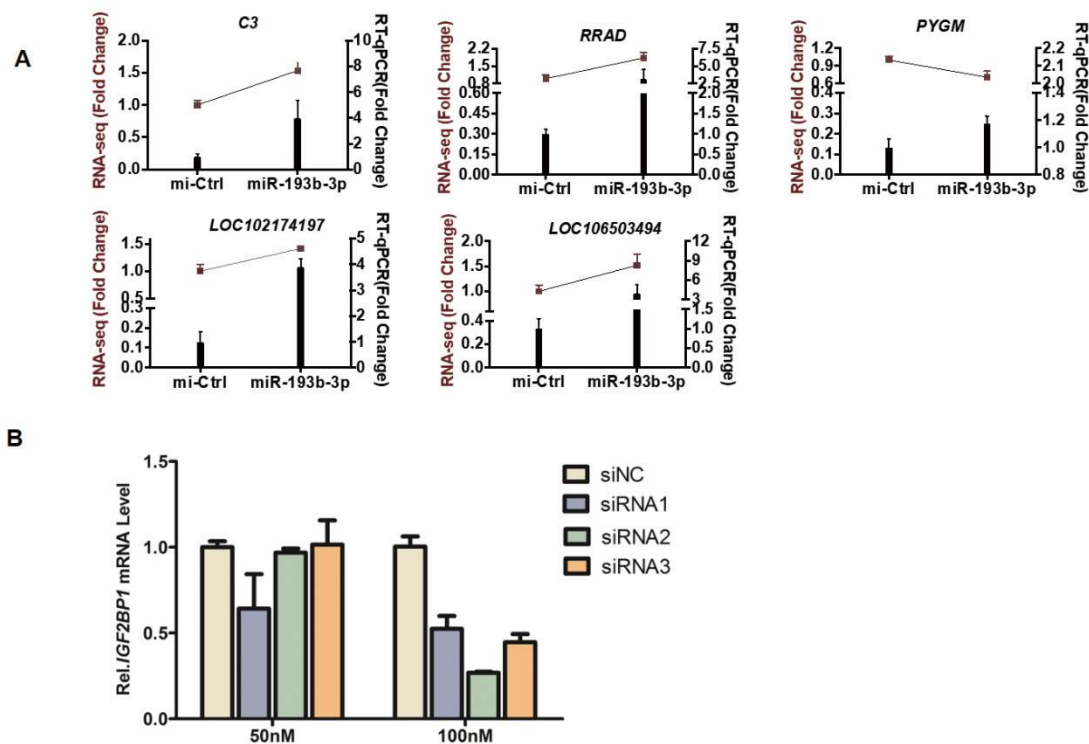
### Supplementary Figure S3 Insulin-like growth factor 2 binding protein 1

**(IGF2BP1) is the most miR-193b-3p-affected insulin genes.**

**(A)** A volcano plot displays  $\log_2foldchange$  ( $\log_2FC$ ) against  $-\log_{10}padj$  from the t-test for all the transcript detected in mRNA-sequencing.

**(B)** Functional enrichment analyses of differential expression genes (DEGs) were implemented using the clusterProfiler R package (v. 3.4.4) with  $Padj < 0.05$ . A red box marks insulin-like growth factor binding (GO:0005520,  $Padj = 0.015$ ).

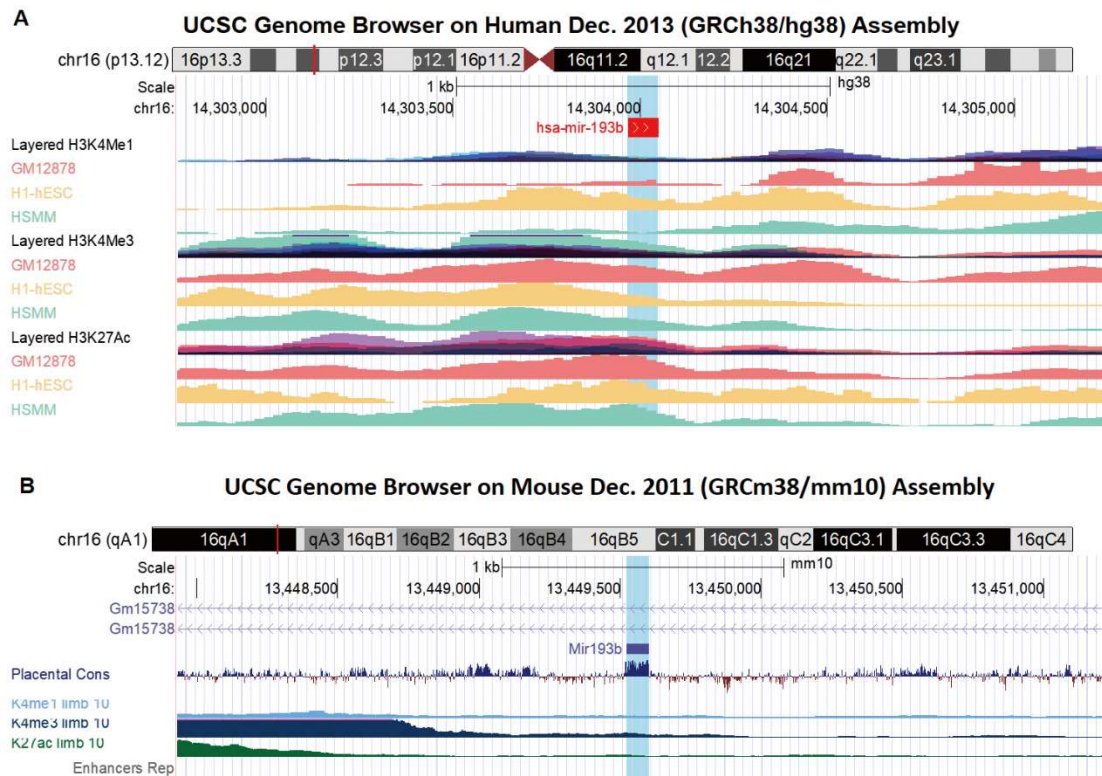
**(C)** A volcano plot for the total 17 insulin family genes detected in RNA-seq. The green dot indicates that gene expression is decreased by miR-193b-3p mimics, while others are elevated compared to mimics control (mi-Ctrl).



**Supplementary Figure S4 qPCR validation of RNA-seq data (A), efficiency of interfering RNAs against IGF2BP1(B).**

**(A)** Validation the abundance of the genes detected in RNA-seq. Data are shown as mean  $\pm$  MSE. C3, Complement C3; RRAD, Ras Associated with Diabetes; PYGM, Glycogen Phosphorylase, Muscle Associated; LOC102174197, xaa-Pro aminopeptidase 2; LOC106503494, H1.2 linker histone.

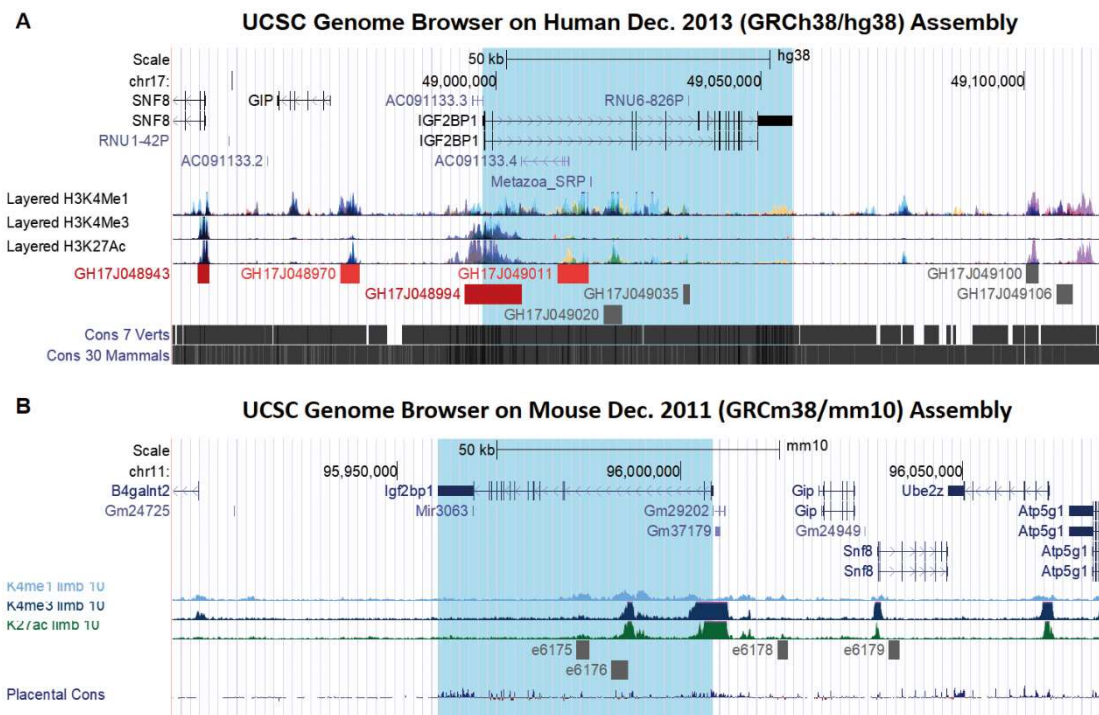
**(B)** Efficiency of siRNAs against IGF2BP1 mRNA. IGF2BP1 abundance in at least three independent samples is quantified via RT-qPCR and calculated using the  $2^{-\Delta\Delta C_t}$ , with  $\beta$ -actin (ACTB) as an internal control and values of control (siNC) set to 1.



**Supplementary Figure S5 Difference of histone modification between human and mouse mir193b loci.**

**(A)** Hsa-mir-193b sits in the peak and valley of H3K4Me1/H3K4me3/ H3K27ac derived from 3 cell lines, including GM12878 (a lymphoblastoid cell line), H1-hESC (H1 human embryonic stem cells), and HSMM (human skeletal muscle myoblasts), in ENCODE UCSC, respectively.

**(B)** Histone modification of mmu-mir-193b gene region in mouse tissues in ENCODE UCSC.



**Supplementary Figure S6 Histone modification of human and mouse IGF2BP1 loci.** Blue lines highlight IGF2BP1 gene region. Both human (A) and mouse (B) IGF2BP1 3' UTR sits in the valley of H3K4Me3 and H3K27Ac.





**Supplementary Figure S7 Location of miR-193b and miR-365 is differed among species in UCSC.** Blue lines highlight hsa-mir-193b and hsa-mir-365a. Yellow arrows mark animals containing miR193 conserve with hsa-mir-193b but lack miR365, while green arrows mark species containing conserve miR365 but lack miR193 on the same chromosome.